Simulating Lossy Interconnect with High Frequency Nonidealities in Linear Time*

Jaijeet S. Roychowdhury A. Richard Newton Donald O. Pederson

Department of Electrical Engineering and Computer Sciences
University of California, Berkeley

Abstract

Transient simulation of lossy lines with high frequency nonidealities (such as skin effect) is usually performed by convolution, which involves computation quadratic in the number of time-points in the simulation. In this paper, a linear time simulation technique is described in which each impulse response is decomposed into two terms, with widely separated rates of decay. One term corresponds to a "simple lossy" line (a line with frequency-independent electrical parameters), while the other represents the contribution of the high frequency nonideality. The latter term can decay to insignificant levels in an interval much shorter than simulation times of interest, making truncation possible and leading to computation in linear time. The former term usually decays over much longer intervals, so truncation is not generally feasible. However, this term is also computed in linear time by a recursive procedure that involves no approximation of impulse responses. Experimental results verify the linear complexity of the new technique and demonstrate computational advantage for simulations of 5 or more cycles, with speedups of more than 10 times for long simulations.

1 Introduction

Efficient transient simulation of lossy transmission lines within nonlinear circuits has recently become a prominent problem. A major application is in the simulation of multi-chip modules (MCMs), high-performance packages that contain long thin interconnections connecting chips. At the high operating speeds of MCMs, interconnections exhibit transmission line effects like reflection, attenuation and dispersion, which can seriously degrade signal quality.

For many applications, transmission lines characterized by constant resistance, inductance, and capacitance (R_{lf}, L_{lf} and C_{lf}) per unit length ("simple lossy lines") are adequate for accurate simulation. At very fast rise times, however, it can be necessary to model these parameters as varying with frequency to account for nonideal effects ("frequency-varying models"). For several nonideal effects, the parameters differ from R_{lf}, L_{lf} and C_{lf} only at high frequencies (hence the term "high frequency nonidealities"). The most important phenomenon requiring frequency-varying models is skin effect, a high frequency nonideality that causes current to concentrate near the surface of the interconnect at high frequencies, thereby increasing the effective resistance. Skin effect can become significant in typical MCM interconnect at rise times less than 1ns[1], rounding off rising and falling edges (*skin effect induced dispersion* [1]).

Many techniques exist for the simulation of transmission line models within nonlinear circuits (see Section 2 for a brief review). The most accurate time domain technique for the simulation of lines with high frequency nonidealities is direct convolution, but this requires computation that rises quadratically with the number of time-points in the simulation. Existing schemes that reduce the complexity to linear rely on assuming specific forms for impulse responses (such as sums of exponentials in the time domain, or rational functions in the frequency domain).

In this work, the impulse responses of frequency-varying lines are first decomposed into two parts, one the response of a simple lossy line, the other the contribution of the nonideality. Second, the fact that the physical mechanisms of *high frequency* nonidealities operate in time scales that are short relative to time scales of interest in practical MCM applications is exploited. This translates to quickly decaying responses for the nonideal part, making truncation, and hence computation in linear time, possible. Truncation is not generally feasible for the responses of the simple lossy line part which can decay slowly. It is shown that the convolution operations involved in the simple lossy part of the computation can be avoided, replaced by a linear time recursive computation which involves no approximation of impulse responses. The validity of the recursive procedure does not follow immediately from our earlier work [2] (the state-based method)[2]. The addition of nonideal terms changes relationships between waveforms that were part of the basis of the recursive formulation for the simple lossy case[3].

Apart from linear complexity, this technique has the advantage of not assuming specific forms for the nonideal responses. Models of differing levels of sophistication exist for nonideal behaviour [3, 1, 4, 5], with responses that differ in the details but share the same time scale. The approach presented here is capable of simulating any such model, including empirically measured data characterising nonidealities. Detailed knowledge of internal physical mechanisms is not required; phenomena such as skin effect that arise from non-uniform current or voltage distributions along the transverse dimensions of the line can be simulated without keeping track of the transverse variation. The price paid for this generality is convolution with the nonideal response; however, exploiting the short time scale of the phenomena generating this response makes computation in linear time possible. For the impulse responses of the simple lossy line, the time scale is not short; for this part, knowledge of the internal mechanism is exploited for efficient simulation, through the recursive state-based technique. This is not restrictive because this internal mechanism is fundamental to all models of transmission lines. All features of the state-based technique for simple lossy lines, like dynamic allocation of sample points for the state (see [2]), apply fully to the the recursive computation part of the nonideal line.

In Section 2, previous approaches to lossy line simulation are reviewed. Section 3 contains the mathematical details of the decomposition and recursive computation. Experimental results are presented in Section 4.

*This research was supported by AT&T Bell Laboratories, IBM, Raytheon and the California State MICRO program.

[1] Other high frequency nonidealities such as dielectric loss [1] can usually be ignored for typical MCM packages.

[2] The state-based method is a linear time recursive procedure for simple lossy lines, i.e., lines *without* nonidealities.

[3] If the transmission line equations are expressed in the admittance, impedance or hybrid representations (i.e., two of the port variables can be clearly identified as "outputs" and the other two as "inputs"), the validity of the recursive procedure follows immediately from our previous work. Using these representations, however, results in impulse responses for the nonideal term that are not eventually monotonically decreasing, and truncation is not possible. Another seemingly workable approach is to precondition the port variables of a simple lossy line such that the preconditioned system is equivalent to a frequency-varying line. This approach is not feasible in a time-stepping simulator because the preconditioning operation can involve convolution with non-causal responses. This work (in Section 3) justifies recursion in the scattering-parameter representation (in which the impulse responses do decay monotonically) with nonidealities.

2 Previous Work

The convolution approach is the most accurate and general approach for the time domain simulation of nonideal lossy lines within nonlinear circuits. ([6, 7] contain descriptions of other methods for lossy line simulation.) Liu et al [8] were apparently first to use convolution to simulate devices similar to lines, i.e., antennas, in conjunction with nonlinear loads. Djordjević et al [9] applied the technique to simulate lossy lines. That the lossy line is a linear two-port was exploited by expressing the "outputs" of the two-port as a convolution of the "inputs" with impulse responses (or Green's functions) characteristic of the line. In a comparison of techniques for lossy line simulation [6], convolution was found slow and only slightly more accurate than the approaches involving lumped approximations. In the early formulation, the duration and nature of the impulse responses was a limitation: for lossless lines, the impulse responses were infinite in duration and consisted of periodic sharp spikes; those of lossy lines diminished gradually while being otherwise similar. Impulse responses that fall to negligible levels after a short time are desirable for computational efficiency[4]. Augmenting the line with a quasi-matched load was attempted in [9] to shorten the responses. Schutt-Aine et al [10, 11] reformulated the convolution equations using a scattering parameter approach that led to "well behaved" impulse responses[5]. Even though these responses decreased monotonically, their effective duration (depending on the values of R, L, G, and C) could be greater than the total simulation time, leading to quadratic complexity. Approaches reducing this complexity to linear have relied mainly on assuming specific functional forms for the impulse responses. Semlyen et al [12] have used sums of exponentials for time domain approximation, while frequency domain simplifications using rational function and Padé approximations [13, 14], essentially translating to exponentials in the time domain, are available. A different approach to linear complexity applicable only to simple lossy lines (the state-based method, [2]) was proposed recently by the present authors. This technique is equivalent to convolution in accuracy and does not involve any approximation of impulse responses.

3 State-Based Formulation with Nonideal Convolution Terms

For a frequency-varying transmission line with parameters $R(s)$, $L(s)$, $C(s)$ and $G(s)$[6], the constitutive equations are[15]:

$$\left[Y_0 V_2(s) H_Y(s) - I_2(s)\right] - \left[Y_0 V_1(s) H_{\gamma Y}(s) + I_1(s) H_\gamma(s)\right] = 0 \quad (1)$$

$$\left[Y_0 V_2(s) H_{\gamma Y}(s) + I_2(s) H_\gamma(s)\right] - \left[Y_0 V_1(s) H_Y(s) - I_1(s)\right] = 0 \quad (2)$$

where $V_1(s)$, $V_2(s)$, $I_1(s)$ and $I_2(s)$ are the Laplace transforms of the voltages and currents at the two ends of the line, which is of length l, and

$$Y_0 = \sqrt{\frac{C_{lf}}{L_{lf}}}, \quad H_Y(s) = \frac{Y(s)}{Y_0}, \quad H_\gamma(s) = e^{-\lambda(s) l} \quad (3)$$

$$H_{\gamma Y}(s) = H_Y(s) H_\gamma(s), \quad Y(s) = \sqrt{\frac{sC(s) + G(s)}{sL(s) + R(s)}} \quad (4)$$

$$\lambda(s) = \sqrt{\left(sC(s) + G(s)\right)\left(sL(s) + R(s)\right)}, \quad (5)$$

$$R_{lf} = R(0), \quad L_{lf} = L(0) \quad (6)$$

$$C_{lf} = C(0), \quad G_{lf} = G(0) \quad (7)$$

Inverse Laplace transformation yields the time domain constitutive equations:

$$\left[Y_0 v_2(t) * h_Y(t) - i_2(t)\right] - \left[Y_0 v_1(t) * h_{\gamma Y}(t) + i_1(t) * h_\gamma(t)\right] = 0 \quad (8)$$

$$\left[Y_0 v_2(t) * h_{\gamma Y}(t) + i_2(t) * h_\gamma(t)\right] - \left[Y_0 v_1(t) * h_Y(t) - i_1(t)\right] = 0 \quad (9)$$

where $*$ is the convolution operator[7], $v_1(t)$, $v_2(t)$, $i_1(t)$, $i_2(t)$ are the port variables of the line, and $h_Y(t)$, $h_\gamma(t)$ and $h_{\gamma Y}(t)$ are the inverse Laplace transforms of $H_Y(s)$, $H_\gamma(s)$ and $H_{\gamma Y}(s)$, respectively.

The above convolution formulation can be used directly to simulate the frequency-varying line. However, it is convenient to rewrite Equations 1 and 2 in the following equivalent form for the purposes of the decomposition mentioned in Section 1:

$$\left[Y_0 V_2(s) H_Y^{lf}(s) - I_2(s)\right] - \left[Y_0 V_1(s) H_{\gamma Y}^{lf}(l,s) + I_1(s) H_\gamma^{lf}(l,s)\right] + U_1(s) = 0 \quad (10)$$

$$\left[Y_0 V_2(s) H_{\gamma Y}^{lf}(l,s) + I_2(s) H_\gamma^{lf}(l,s)\right] - \left[Y_0 V_1(s) H_Y^{lf}(s) - I_1(s)\right] + U_2(s) = 0 \quad (11)$$

where:

$$H_Y^{lf}(s) = \frac{Y^{lf}(s)}{Y_0}, \quad H_\gamma^{lf}(x,s) = e^{-\lambda^{lf}(s) x} \quad (12)$$

$$H_{\gamma Y}^{lf}(x,s) = H_Y^{lf}(s) H_\gamma^{lf}(x,s), \quad Y^{lf}(s) = \sqrt{\frac{sC_{lf} + G_{lf}}{sL_{lf} + R_{lf}}} \quad (13)$$

$$\lambda^{lf}(s) = \sqrt{\left(sC_{lf} + G_{lf}\right)\left(sL_{lf} + R_{lf}\right)} \quad (14)$$

$U_1(s)$ and $U_2(s)$ represent the contribution of the frequency-varying part of the line:

$$U_1(s) = \left[Y_0 V_2(s) \triangle H_Y(s)\right] - \left[Y_0 V_1(s) \triangle H_{\gamma Y}(s) + I_1(s) \triangle H_\gamma(s)\right] \quad (15)$$

$$U_2(s) = \left[Y_0 V_2(s) \triangle H_{\gamma Y}(s) + I_2(s) \triangle H_\gamma(s)\right] - \left[Y_0 V_1(s) \triangle H_Y(s)\right] \quad (16)$$

where:

$$\triangle H_Y(s) = H_Y(s) - H_Y^{lf}(s), \quad \triangle H_\gamma(s) = H_\gamma(s) - H_\gamma^{lf}(l,s) \quad (17)$$

$$\triangle H_{\gamma Y}(s) = H_{\gamma Y}(s) - H_{\gamma Y}^{lf}(l,s) \quad (18)$$

Laplace inversion of Equations 10 and 11 yields the time domain formulation:

$$\left[Y_0 v_2(t) * h_Y^{lf}(t) - i_2(t)\right] - \left[Y_0 v_1(t) * h_{\gamma Y}^{lf}(l,t) + i_1(t) * h_\gamma^{lf}(l,t)\right] + u_1(t) = 0 \quad (19)$$

$$\left[Y_0 v_2(t) * h_{\gamma Y}^{lf}(l,t) + i_2(t) * h_\gamma^{lf}(l,t)\right] - \left[Y_0 v_1(t) * h_Y^{lf}(t) - i_1(t)\right] + u_2(t) = 0 \quad (20)$$

where $h_Y^{lf}(t)$, $h_\gamma^{lf}(x,t)$ and $h_{\gamma Y}^{lf}(x,t)$[8] are the inverse Laplace transforms of $H_Y^{lf}(s)$, $H_\gamma^{lf}(x,s)$ and $H_{\gamma Y}^{lf}(x,s)$ respectively. $u_1(t)$ and $u_2(t)$, the inverse transforms of $U_1(s)$ and $U_2(s)$, are given by:

[4] If the responses remain significant for a period greater than the total simulation time, convolution from time $t_0 = 0$ to $t = t_n$ is necessary at every time-point t_n. This operation requires computation proportional to n, resulting in total computation proportional to N^2 (quadratic time complexity) in a simulation with N time-points.

[5] The "well behaved" impulse response for a lossless line is a single Dirac delta function at the line delay; for lossy lines, the impulse responses decrease asymptotically and monotonically to zero.

[6] s denotes the Laplace variable (= $j2\pi f$ for the Fourier transform).

[7] $a(t) * b(t) = \int_0^t a(\tau)\, b(t-\tau)\, d\tau$.

[8] Analytic expressions for these are given later in this section.

$$u_1(t) = \left[Y_0\, v_2(t) * \triangle h_\Upsilon(t)\right] - \left[Y_0\, v_1(t) * \triangle h_{\gamma\Upsilon}(t) + i_1(t) * \triangle h_\gamma(t)\right] \quad (21)$$

$$u_2(t) = \left[Y_0\, v_2(t) * \triangle h_{\gamma\Upsilon}(t) + i_2(t) * \triangle h_\gamma(t)\right] - \left[Y_0\, v_1(t) * \triangle h_\Upsilon(t)\right] \quad (22)$$

where

$$\triangle h_\Upsilon(t) = h_\Upsilon(t) - h_\Upsilon^{lf}(t), \quad \triangle h_\gamma(t) = h_\gamma(t) - h_\gamma^{lf}(l,t) \quad (23)$$

$$\triangle h_{\gamma\Upsilon}(t) = h_{\gamma\Upsilon}(t) - h_{\gamma\Upsilon}^{lf}(l,t) \quad (24)$$

Equations 19 and 20 are equivalent to Equations 8 and 9. The motivation behind rewriting the latter equations as the former stems from that all terms except u_1 and u_2 can be computed recursively, as shown later in this section. Calculating $u_1(t)$ and $u_2(t)$ (according to Equations 21 and 22) requires convolution; if, however, the responses $\triangle h_\Upsilon$, $\triangle h_\gamma$ and $\triangle h_{\gamma\Upsilon}$ can be truncated with insignificant loss of accuracy (as in the high frequency nonidealities being considered), convolution transforms into an integral with fixed limits.

The existing formulation of the state-based method [2] is applicable only to the dc-parameter case, for which the constitutive equations are (Equations 19 and 20 with $u_1(t) = u_2(t) \equiv 0$):

$$\left[Y_0\, v_2(t) * h_\Upsilon^{lf}(t) - i_2(t)\right] - \left[Y_0\, v_1(t) * h_{\gamma\Upsilon}^{lf}(l,t) + i_1(t) * h_\Upsilon^{lf}(l,t)\right] = 0 \quad (25)$$

$$\left[Y_0\, v_2(t) * h_{\gamma\Upsilon}^{lf}(l,t) + i_2(t) * h_\gamma^{lf}(l,t)\right] - \left[Y_0\, v_1(t) * h_\Upsilon^{lf}(t) - i_1(t)\right] = 0 \quad (26)$$

The state-based method, as derived in [2], asserts that Equations 25 and 26 are equivalent to a different set of equations that do not use convolution but involve an internal state term. Thus the expressions on the LHS of Equations 25 and 26 are in essence computed in a recursive manner, without using past values of v_1, v_2, i_1 and i_2. *Implicit in this procedure is the assumption that $v_1(t)$, $v_2(t)$, $i_1(t)$ and $i_2(t)$ are constrained to obey Equations 25 and 26 at any t. If this assumption does not hold (as in Equations 19 and 20 with nonzero $u_1(t)$ and $u_2(t)$), then it does not automatically follow from [2] that the recursive procedure is still equivalent to the LHS of Equations 25 and 26.*

In this work, it is proved that the recursive computation of the state-based procedure is always equivalent to the LHS of Equations 25 and 26, i.e., for *arbitrary* $v_1(t)$, $v_2(t)$, $i_1(t)$ and $i_2(t)$. A set of partial differential equations (PDEs) are constructed such that their solution yields Equations 19 and 20. An alternative solution procedure that replaces all terms except $u_1(t)$ and $u_2(t)$ by a recursive computation is developed. Then the fact that the PDEs must have a unique solution given a unique set of external influences is used to assert the equivalence of the recursive procedure and the LHS of Equations 25 and 26. The key difference between this procedure and the one in [2] is the addition of terms w_1 and w_2 (see Equations 27 and 28 in the next paragraph) that are contributed by the nonideality. While these terms do not admit of any obvious physical interpretation, their inclusion leads to both the nonideal convolution equations (Equations 19 and 20) and the recursive technique for the simple lossy line part. As mentioned earlier, attempts to introduce the nonideal term through the port variables and formulations other than the scattering-parameter one lead to noncausal situations or destroy the quickly decaying property of the purely nonideal responses.

Let $w_1(x,t)$ and $w_2(x,t)$ be two arbitrary functions defined on $[0,l] \times [0,\infty)$. Consider the following (the familiar Telegrapher Equations [11] with "inputs"[9] w_1 and w_2):

$$\frac{\partial v}{\partial x} = -\left(L_{lf}\frac{\partial i}{\partial t} + R_{lf}\, i\right) + w_1 \quad (27)$$

[9]Not to be confused with the port variables.

$$\frac{\partial i}{\partial x} = -\left(C_{lf}\frac{\partial v}{\partial t} + G_{lf}\, v\right) + w_2 \quad (28)$$

The above equations hold for x varying between 0 and l, the length of the transmission line. $v(x,t)$ and $i(x,t)$ are the voltage and current at the point x in the line at time t, respectively. It is assumed that the simulation starts from time 0.

The circuit interacts with the transmission line through the port variables $v_1(t) = v(0,t)$, $i_1(t) = i(0,t)$, $v_2(t) = v(l,t)$ and $i_2(t) = -i(l,t)$. These four port variables specify the *boundary conditions* of Equations 27 and 28.

In addition to w_1, w_2, and the port variables, the internal state of the transmission line also determines the future behaviour of the line. This internal state is stored in the energy-storing distributed inductance and capacitance and is specified by the voltages and currents in the line's interior at time 0, $v_0(x) = v(x,0)$ and $i_0(x) = i(x,0)$. $v_0(x)$ and $i_0(x)$ are the *initial conditions* for Equations 27 and 28. The combination of the Telegrapher Equations, the boundary and initial conditions and the "inputs" w_1 and w_2 specify the future behaviour of the line uniquely.

Equations 27 and 28 are solved to obtain time domain relations between w_1, w_2, $v(x,t)$, $i(x,t)$ and the internal state $v_0(x)$, $i_0(x)$. (The derivation is omitted for brevity; see [16] for the details.) In the process, w_1 and w_2 are chosen as functions of u_1 and u_2 (of Equations 21 and 22). Moreover, the state $v_0(x)$, $i_0(x)$ is represented by samples v_{0j}, i_{0j} at points x_j, $j = 1, \ldots, n_t$, inside the line. n_t is the total number of state samples; the index of a sample point at x is denoted by n_x, with $n_0 = 1$. The time domain equations finally obtained for the nonideal line, valid at any $x \in [0,l]$, are:

$$\left[Y_0\, v(x,t) * h_\Upsilon^{lf}(t) + i(x,t)\right] - \left[Y_0\, v(0,t) * h_{\gamma\Upsilon}^{lf}(x,t) + i(0,t) * h_\gamma^{lf}(x,t)\right] + u_1(t)\,\chi(x-l) = \sum_{j=1}^{n_x} \left\{ \begin{array}{l} i_{0j}\left[h_{S\gamma\Upsilon}(x - x_j, t) - h_{S\gamma\Upsilon}(x - x_{j-1}, t)\right] + \\ Y_0\, v_{0j}\left[h_{S\gamma}(x - x_j, t) - h_{S\gamma}(x - x_{j-1}, t)\right] \end{array} \right\} \quad (29)$$

$$\left[Y_0\, v(l,t) * h_{\gamma\Upsilon}^{lf}(l-x,t) - i(l,t) * h_\gamma^{lf}(l-x,t)\right] - \left[Y_0\, v(x,t) * h_\Upsilon^{lf}(t) - i(x,t)\right] + u_2(t)\,\chi(x) = \sum_{j=n_x}^{n_t} \left\{ \begin{array}{l} i_{0j}\left[h_{S\gamma\Upsilon}(x_{j-1} - x, t) - h_{S\gamma\Upsilon}(x_j - x, t)\right] \\ -Y_0\, v_{0j}\left[h_{S\gamma}(x_{j-1} - x, t) - h_{S\gamma}(x_j - x, t)\right] \end{array} \right\} \quad (30)$$

where:

$$h_\Upsilon(t) = \left[\delta(t) + \alpha\{I_1(\alpha t) - I_0(\alpha t)\}\right] e^{-\beta t} \quad (31)$$

$$h_\gamma(x,t) = \left[\delta(t - \gamma_0 x) + u(t - \gamma_0 x)\frac{\alpha\gamma_0 x\, I_1\left(\alpha\sqrt{t^2 - (\gamma_0 x)^2}\right)}{\sqrt{t^2 - (\gamma_0 x)^2}}\right] e^{-\beta t} \quad (32)$$

$$h_{\gamma\Upsilon}(x,t) = \left[\delta(t - \gamma_0 x) + u(t - \gamma_0 x)\,\alpha \times \left\{\frac{t I_1\left(\alpha\sqrt{t^2 - (\gamma_0 x)^2}\right)}{\sqrt{t^2 - (\gamma_0 x)^2}} - I_0\left(\alpha\sqrt{t^2 - (\gamma_0 x)^2}\right)\right\}\right] e^{-\beta t} \quad (33)$$

$$h_{S\gamma}(x,t) = u(t - \gamma_0 x)\, I_0\left(\alpha\sqrt{t^2 - (\gamma_0 x)^2}\right) e^{-\beta t} \quad (34)$$

$$h_{S\gamma Y}(x,t) = u(t-\gamma_0 x)\left[e^{-\alpha(t-\gamma_0 x)} + \alpha\gamma_0 x \int_{\gamma_0 x}^{t} e^{-\alpha(t-\tau)} \frac{I_1\left(\alpha\sqrt{\tau^2-(\gamma_0 x)^2}\right)}{\sqrt{\tau^2-(\gamma_0 x)^2}} d\tau \right] e^{-\beta t} \quad (35)$$

In the above, $u(\cdot)$ and $\delta(\cdot)$ denote the unit step and delta functions, respectively. $\chi(x)$ is defined to be 1 if $x = 0$, 0 otherwise.

The equations obtained by substituting $x = l$ in Equation 29 and $x = 0$ in Equation 30 are of special interest:

$$\begin{aligned}&\left[Y_0 v_2(t) * h_Y^{lf}(t) - i_2(t)\right] - \left[Y_0 v_1(t) * h_{\gamma Y}^{lf}(l,t) + i_1(t) * h_Y^{lf}(l,t)\right] + u_1(t) \\ &= \sum_{j=1}^{n_l} \left\{ \begin{array}{l} i_{0j}\left[h_{S\gamma Y}(l-x_j,t) - h_{S\gamma Y}(l-x_{j-1},t)\right] + \\ Y_0 v_{0j}\left[h_{S\gamma}(l-x_j,t) - h_{S\gamma}(l-x_{j-1},t)\right] \end{array} \right\} \end{aligned} \quad (36)$$

$$\begin{aligned}&\left[Y_0 v_2(t) * h_{\gamma Y}^{lf}(l,t) + i_2(t) * h_Y^{lf}(l,t)\right] - \left[Y_0 v_1(t) * h_Y^{lf}(t) - i_1(t)\right] + u_2(t) \\ &= \sum_{j=1}^{n_l} \left\{ \begin{array}{l} i_{0j}\left[h_{S\gamma Y}(x_{j-1},t) - h_{S\gamma Y}(x_j,t)\right] \\ -Y_0 v_{0j}\left[h_{S\gamma}(x_{j-1},t) - h_{S\gamma}(x_j,t)\right] \end{array} \right\} \end{aligned} \quad (37)$$

The above are the equations of the convolution technique with an additional RHS term from the initial state. At the start of the simulation, the initial state is assumed zero[10]. The RHS then becomes zero, and the two equations become identical to Equations 19 and 20, which, by construction, are equivalent to Equations 8 and 9. These equations may be used directly for simulation by convolution: at time-point t_i, each convolution on the LHS is carried out from $t_0 = 0$ to t_i, using stored values of v_1, v_2, i_1 and i_2 at t_j for all j, $0 \le j < i$. The computation required at each t_i is proportional to i, leading to the quadratic complexity property.

The fact that Equations 36 and 37 are derived from a system of PDEs makes it possible to solve them in another way: at time t_1 (the first time-point after $t_0 = 0$), the procedure is identical to the convolution method, with convolution over the interval $[t_0, t_1]$, and initial state zero. The new state of the line at time t_1 is calculated next, using Equations 29 and 30 for each x chosen to sample the internal state. At the next time-point t_2, the newly calculated, nonzero internal state at t_1 is used as $v_0(x)$ and $i_0(x)$, instead of the zero internal state at time t_0, in Equations 29, 30, 36 and 37. In other words, the time-invariance property of the Telegrapher Equations is used. Thus the convolution operation at time t_2 starts from the previous time-point t_1, i.e., the time at which the internal state is used in the above equations, instead of from t_0 as in the convolution method. The internal state at t_2 is then calculated, and this internal state is used as the initial state at time t_3, and so on. This procedure is the basis of the recursive computation; information from the port variables' history, which keeps increasing in size as the simulation progresses, is condensed into the state, which is of constant size. The key feature leading to linear complexity in this technique is that the computation at time t_i is independent of i, since convolution is always performed over only one interval, $[t_{i-1}, t_i]$.

This recursive procedure is valid for arbitrary $u_1(t)$ and $u_2(t)$, not just the particular choices of Equations 21 and 22. The validity of the recursion in computing the LHS of Equations 25 and 26 for arbitrary $v_1(t)$, $v_2(t)$, $i_1(t)$ and $i_2(t)$ follows immediately.

4 Experimental Results

The techniques outlined in the previous section were implemented in the circuit simulator SPICE3 version 3e1 [17]. Results on an example circuit with typical MCM interconnect are presented in this section.

The physical parameters of the aluminium interconnect (taken from [18]) are: width = 11μm, thickness = 2μm, height above ground plane = 10μm, SiO_2 dielectric, length of line = 10cm, R_{lf} = 12 ohms/cm, L_{lf} = 8.79 nH/cm, C_{lf} = 1 pF/cm. Dielectric loss (parallel conductance G) is assumed to be zero at all frequencies. Skin effect is accounted for with the following model [1]:

$$R(f) = \left\{ \begin{array}{ll} R_0\sqrt{f} & f \ge f_T \\ R_{lf} & f < f_T \end{array} \right. \quad (38)$$

$$L(f) = \left\{ \begin{array}{ll} L_{ext} + \frac{L_0}{\sqrt{f}} & f \ge f_T \\ L_{lf} & f < f_T \end{array} \right. \quad (39)$$

$C(f)$ is assumed constant at C_{lf}; f_T, the transition frequency after which skin effect becomes significant, is taken to be 1 GHz from [1]; L_{ext}, the inductance external to the wire and less than L_{lf}, is assumed to be 4 nH/cm. From these, R_0 and L_0 are calculated to be 3.7947×10^{-4} and 1.5147×10^{-4} respectively. The ideal delay $T = l\sqrt{L_{lf} C_{lf}}$ is 0.9375 ns.

The impulse responses of the pure nonideality Δh_Y, Δh_γ and $\Delta h_{\gamma Y}$ contain impulse (delta function) components which are first separated out. $\Delta h'_Y$, $\Delta h'_\gamma$ and $\Delta h'_{\gamma Y}$, the components without impulses, were calculated by numerical inversion of the Fourier transform, and are shown in Figs. 1, 2 and 3. The following relations hold:

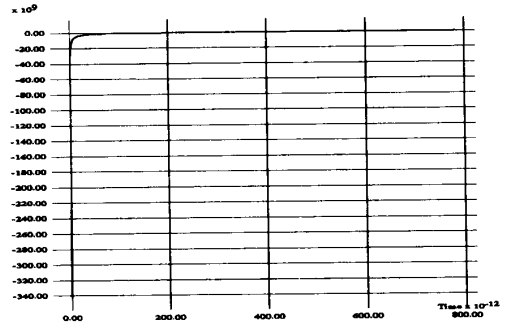

Figure 1: $\Delta h'_Y(t)$

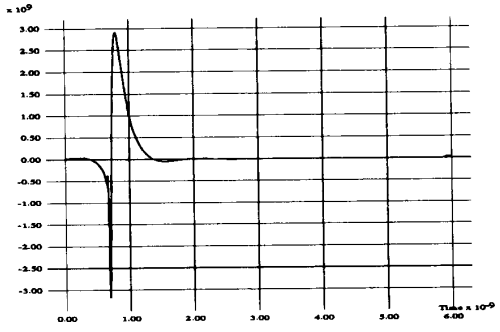

Figure 2: $\Delta h'_\gamma(t)$

[10] If the circuit is at a nonzero DC initial state, a simple reformulation exploiting the linearity of the transmission line yields a system with zero initial state.

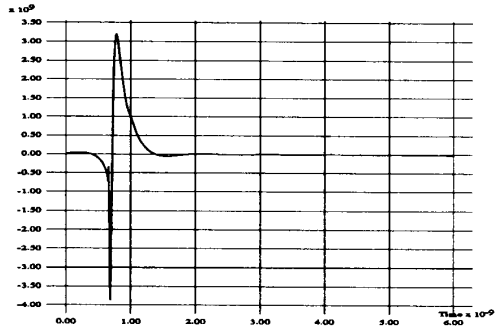

Figure 3: $\Delta h'_{\gamma\Upsilon}(t)$

$$\Delta h_\Upsilon(t) = M_\Upsilon\,\delta(t) + \Delta h'_\Upsilon(t) \quad (40)$$

$$\Delta h_\gamma(t) = M_\gamma\,\delta(t-T) + \Delta h'_\gamma(t) \quad (41)$$

$$\Delta h_{\gamma\Upsilon}(t) = M_{\gamma\Upsilon}\,\delta(t-T) + \Delta h'_{\gamma\Upsilon}(t) \quad (42)$$

For this example, $M_\Upsilon = 0.420210266, M_\gamma = -0.5326360212$, and $M_{\gamma\Upsilon} = -0.5160118569$. In order to obtain a quantitative estimate of the error caused by truncation, the functions $\int_0^t \Delta h'_\Upsilon(\tau)\,d\tau$, $\int_0^t \Delta h'_\gamma(\tau)\,d\tau$, and $\int_0^t \Delta h'_{\gamma\Upsilon}(\tau)\,d\tau$ are useful. Plots of these functions for this example are shown in Figs. 4, 5 and 6; the point after which these functions achieve a steady value is the effective length of the response.

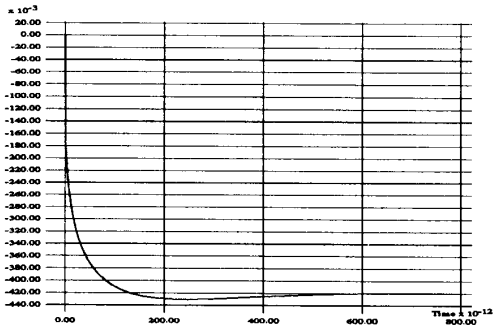

Figure 4: $\int_0^t \Delta h'_\Upsilon(\tau)\,d\tau$

For this example, the effective durations of $\Delta h'_\Upsilon$, $\Delta h'_\gamma$ and $\Delta h'_{\gamma\Upsilon}$ were 600ps, 3ns and 3ns respectively, as seen from the plots of their integrals. Convolution was performed using the numerical formula in [15].

The circuit consisted of a nonlinear load of two clamping diodes driven by a voltage source with a series resistance through the lossy line. Rise times of 10ps and 1ns were used.

Fig. 7 illustrates the voltage at the load end for the 10ps rise-time case. Simulation by pure convolution and the state-based/conv. technique of this paper are seen to yield identical results. Also shown is the result of simulation without skin effect, i.e., with only DC losses considered. The rise time degradation caused by skin effect, and the rounding of edges, can be seen clearly.

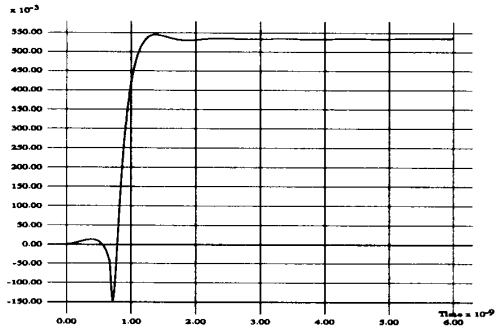

Figure 5: $\int_0^t \Delta h'_\gamma(\tau)\,d\tau$

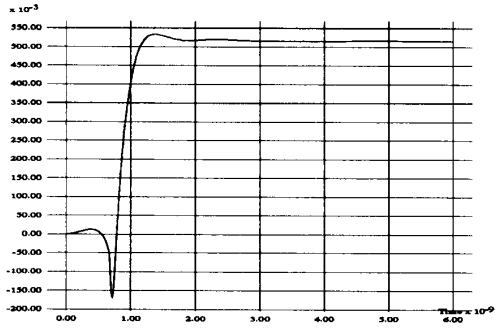

Figure 6: $\int_0^t \Delta h'_{\gamma\Upsilon}(\tau)\,d\tau$

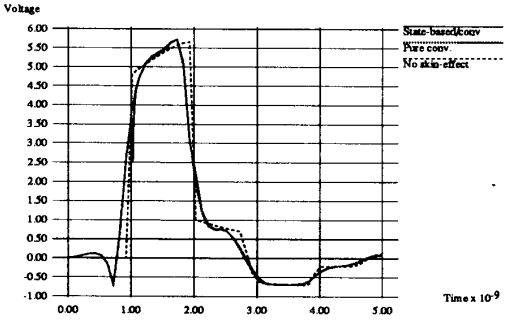

Figure 7: Load voltage, 10ps rise time

Fig. 8 shows the load voltage for a rise time of 1ns. It is seen that skin effect makes virtually no difference to the waveform in this case.

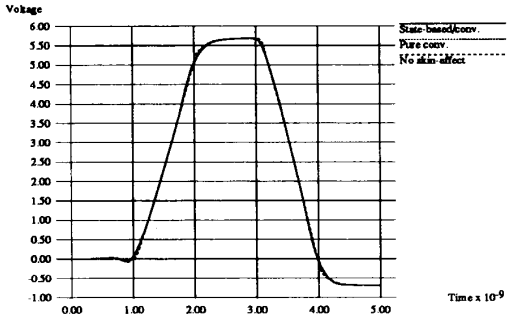

Figure 8: Load voltage, 1ns rise time

Table 1 and Fig. 9 show computation time as a function of total simulation length for the state-based and the pure convolution techniques. The linear and quadratic complexities of the two methods are apparent from the figure.

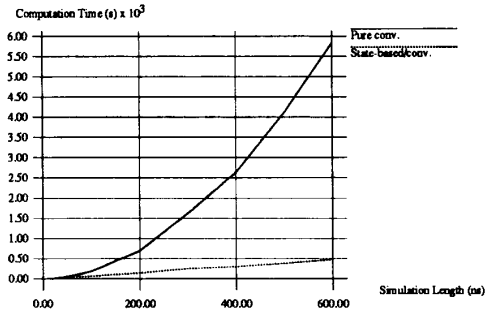

Figure 9: Execution time vs. simulation length

Acknowledgments

Gerry Marino's encouragement and support of this work is greatly appreciated. Technical discussions with Albert Ruehli and Jacob White were very helpful. Thanks are due to Sally Liu and Ta-Fang Fang for encouragement and to Chris Lennard for assistance during implementation and for suggesting the title of this paper. Administrative help from Kia Cooper is very much appreciated.

References

[1] A. Deutsch et al. High-speed signal propagation on lossy transmission lines. *IBM J. Res. Dev.*, 34(4):601–615, July 1990.

[2] J.S. Roychowdhury et al. An Impulse-Response Based Linear Time-Complexity Algorithm for Lossy Interconnect Simulation. In *Proc. IEEE International Conference on Computer Aided Design*, pages 62–65, Santa Clara, CA, November 1991.

[3] H.A. Wheeler. Formulas for the skin effect. *Proc. IRE*, 30:412–424, 1942.

[4] W. Wlodarczyk and V. Besch. Skin-Effect Losses of Interconnect Lines in Frequency and Time-Domain. *Elec. Let.*, 26(16):1237–1238, 2nd August 1990.

Simulation Length	Execution Time[a]	
	State-based/conv.	Convolution only
10 ns	6.82 s	4.90 s
20 ns	13.4 s	12.83 s
40 ns	26.72 s	38.26 s
60 ns	40.35 s	75.8 s
80 ns	53.59 s	126 s
100 ns	70.16 s	186.2 s
200 ns	140.78 s	695 s
300 ns	253.8 s	1619.5 s
400 ns	302.4 s	2635.1 s
500 ns	383.5 s	4110.6 s
600 ns	473.2 s	5839.9 s

[a]CPU times on a DEC 5000/200 running Ultrix 4.2.

Table 1: Comparison of Execution Times

[5] R.A. Sainati and T.J. Moravec. Estimating High Speed Circuit Interconnect Performance. *IEEE Trans. Ckts. Sys.*, 36(4):533–541, April 1990.

[6] A.R. Djordjević et al. Time-Domain Response of Multiconductor Transmission Lines. *Proc. IEEE*, 75(6):743, June 1987.

[7] J.S. Roychowdhury, A. R. Newton, and D.O. Pederson. Algorithms for the Transient Simulation of Lossy Interconnect. Submitted to IEEE Trans. CAD.

[8] T. K. Liu and F. M. Tesche. Analysis of antennas and scatterers with nonlinear loads. *IEEE Trans. Antennas Propagat.*, AP-24:131, March 1976.

[9] A.R. Djordjević et al. Analysis of Lossy Transmission Lines with Arbitrary Nonlinear Terminal Networks. *IEEE Trans. Microwave Th. Tech.*, MTT-34(6):660, June 1986.

[10] J.E. Schutt-Aine and R. Mittra. Scattering Parameter Transient Analysis of Transmission Lines loaded with Nonlinear Terminations. *IEEE Trans. Microwave Th. Tech.*, MTT-36:529–536, 1988.

[11] J.E. Schutt-Aine and R. Mittra. Nonlinear Transient Analysis of Coupled Transmission Lines. *IEEE Trans. Ckts. Sys.*, 36(7), July 1989.

[12] A. Semlyen and A. Dabuleanu. Fast and Accurate Switching Transient Calculations on Transmission Lines with Ground Return Using Recursive Convolution. *IEEE Trans. Power App. Sys.*, PAS-94:561–571, 1975.

[13] F.Y. Chang. Waveform Relaxation Analysis of RLCG Transmission Lines. *IEEE Trans. Ckts. Sys.*, 37(11):1394–1415, November 1990.

[14] S. Lin and E.S. Kuh. Padé Approximation Applied to Transient Simulation of Lossy Coupled Transmission Lines. In *IEEE Multi-Chip Module Conference*, Santa Cruz, CA, March 1992. To appear.

[15] J.S. Roychowdhury and D.O. Pederson. Efficient Transient Simulation of Lossy Interconnect. In *Proc. IEEE Design Automation Conference*, pages 740–745, San Francisco, CA, June 1991.

[16] J.S. Roychowdhury, A. R. Newton, and D.O. Pederson. Simulating Lossy Interconnect with High Frequency Nonidealities in Linear Time. To be submitted to IEEE Trans. CAD.

[17] T.L. Quarles. *Analysis of Performance and Convergence Issues for Circuit Simulation.* PhD thesis, EECS Dept., Univ. Calif., Berkeley, Elec. Res. Lab., April 1989. Memorandum no. UCB/ERL M89/42.

[18] C.A. Neugebauer et al. High Performance Interconnections between VLSI Chips. *Solid State Tech.*, June 1988.